

CHEMISTRY

Revealing the in vivo growth and division patterns of mouse gut bacteria

Liyuan Lin¹, Qiuyue Wu^{1,2}, Jia Song¹, Yahui Du², Juan Gao¹, Yanling Song^{1,2}, Wei Wang^{1*}, Chaoyong Yang^{1,2*}

Current techniques for studying gut microbiota are unable to answer some important microbiology questions, like how different bacteria grow and divide in the gut. We propose a method that integrates the use of sequential D-amino acid–based in vivo metabolic labeling with fluorescence in situ hybridization (FISH), for characterizing the growth and division patterns of gut bacteria. After sequentially administering two D-amino acid–based probes containing different fluorophores to mice by gavage, the resulting dual-labeled peptidoglycans provide temporal information on cell wall synthesis of gut bacteria. Following taxonomic identification with FISH probes, the growth and division patterns of the corresponding bacterial taxa, including species that cannot be cultured separately in vitro, are revealed. Our method offers a facile yet powerful tool for investigating the in vivo growth dynamics of the bacterial gut microbiota, which will advance our understanding of bacterial cytology and facilitate elucidation of the basic microbiology of this gut “dark matter.”

INTRODUCTION

The biological diversity and complexity of the mammalian gut microbiota present formidable obstacles to the investigation and comprehension of these intimate microbial neighbors. To fully comprehend the physiological and pathological functions executed by gut microbiotas, it is critical to understand the basic microbiology of these microbes, such as how different bacteria grow and divide in the gut (1). However, even after nearly two decades of ever-increasing gut microbiota research, many of these questions remain unaddressed (2). The difficulty of separate culture of many gut bacterial species in vitro, which is partially why these microbes are often referred to as the “dark matter” in the gut (3), prevents researchers from further investigating these bacteria in the laboratory. After extensive efforts in optimizing culture conditions for different gut bacteria by microbiologists, gradually more species can be cultured individually in vitro (4). Nonetheless, for the bacteria that can be cultured and investigated in vitro, to what extent the microbial knowledge obtained from in vitro studies can be translated into in vivo situations remains debatable (1). Therefore, a method that can be used to directly probe and investigate the gut microbes in vivo is highly desirable (5).

One approach that could directly probe the indigenous activities of gut microbes uses a traditional isotope-based labeling strategy. N¹⁵-tagged amino acids were given to mice by intravenous injection, and the microbial N¹⁵ signals in the gut acquired by bacterial foraging on host proteins were then detected using nanoscale resolution secondary ion mass spectrometry (6). Consequently, the metabolic activities and host-protein usage preference of different gut bacteria could be assessed. Nonetheless, the data acquisition of

this isotope labeling approach is restricted to the highly specialized mass spectrometry–based technique, and the knowledge obtained was limited to a specific metabolic pathway of the bacteria. A different chemical approach, fluorescent D-amino acid (FDAA)–based metabolic labeling, has been highly valuable in bacteriology studies, because of the labeling specificity [targeting bacterial peptidoglycan (PGN), thus no labeling on eukaryotes], speed (labeling within minutes under optimized conditions), and ease of use (reading fluorescent signals with routine analytical equipment) (7, 8). Recently, it has been demonstrated that FDAA probes could label mouse gut microbiota in vivo with high efficiency, and we further established a STAMP (sequential tagging with D-amino acid–based metabolic probes) strategy for recording the survival of transplanted microbiota in the receiving mouse using the labeling signals of the two FDAA probes (9, 10).

Here, to develop a method that can directly probe and visualize the growth and division modes of different gut bacteria in situ, we propose a STAMP-based and fluorescence in situ hybridization (FISH)–facilitated probing strategy. In this method, two FDAAs with different fluorophores were sequentially administered to mice by gavage to record in vivo bacterial growth and division processes during the labeling period. Consequently, identifying the labeled bacteria with FISH probes at different taxonomic levels (genus and species) allowed us to determine how different bacterial taxa, particularly those that cannot be cultured in vitro, grow and divide in the mammalian gut.

RESULTS

FDAA sequential labeling of mouse gut microbiota

DAAAs are essential building blocks for bacterial PGN synthesis; the sidechain-functionalized DAAAs (i.e., FDAA) are well-tolerated by the enzymes (D, D or L, D-transpeptidases) involved in cell wall construction (7). Chronological use of multiple FDAAs has provided valuable information of the temporal PGN synthesis in several model bacterial species in vitro (10). Here, to study the in vivo growth and division patterns of different bacterial taxa in gut microbiota, we sequentially applied two FDAA probes,

Copyright © 2020
The Authors, some
rights reserved;
exclusive licensee
American Association
for the Advancement
of Science. No claim to
original U.S. Government
Works. Distributed
under a Creative
Commons Attribution
License 4.0 (CC BY).

¹Institute of Molecular Medicine, Shanghai Key Laboratory for Nucleic Acid Chemistry and Nanomedicine, Renji Hospital, Shanghai Jiao Tong University School of Medicine, Shanghai 200127, China. ²The MOE Key Laboratory of Spectrochemical Analysis and Instrumentation, Key Laboratory for Chemical Biology of Fujian Province State Key Laboratory of Physical Chemistry of Solid Surfaces, Department of Chemical Biology, College of Chemistry and Chemical Engineering, Xiamen University, Xiamen 361005, China.

*Corresponding author. Email: wwang@shsmu.edu.cn (W.W.); cyang@xmu.edu.cn (C.Y.)

TAMRA-amino-D-alanine (TADA) and Cy5-amino-D-alanine (Cy5ADA), containing TAMRA (tetramethylrhodamine) or Cy5 (Cyanine 5) on side chains, in two gavages to label the mouse gut microbiota (scheme shown in Fig. 1A). The probes were given at an interval of 3 hours, and the collected cecal microbiota showed strong two-color labeling (Fig. 1B) with high coverage (fig. S1) after 6 hours of the first gavage without apparent alterations of the microbiota composition (fig. S2).

The two-color fluorescence imaging showed a great morphological diversity of the gut microbes. Different distributions of the two colors among various bacteria revealed their distinct dividing patterns and growth rates. Because the second probe used in the sequential labeling was Cy5ADA, the PGN sites with more active constructions had stronger labeling of Cy5 (shown in red), and PGN synthesized earlier had more TAMRA signals (shown in green). Thus, the color distributions of red/green provided a chronological account of the PGN synthesis in each bacterium. Most of the bacteria grew in a dispersed model with relatively strong FDAA labeling throughout the cell (Fig. 1B) and divided in binary fission with one or more red-labeled septums in the middle of the bacteria (Fig. 1C, nos. 1 and 2). Some bacteria were only labeled with the first probe (Fig. 1C, no. 3), suggesting that these cells might have different growth rates during the two labeling steps. It is worth noting that many bacteria showed asymmetric labeling (Fig. 1C, nos. 4 and 5).

Some only had one red pole, with two halves having very different labeling intensities (no. 4). One explanation is that these were the daughter cells from a binary fission, and the red pole was from the newly separated septum. It is also possible that some of these bacteria might grow in an asymmetric or polarized manner, like the zonal-apical growth observed in *Agrobacterium tumefaciens* (7). Moreover, it was also common to see the two daughter cells with different growth rates, where only one of the two cells showed a new septum (Fig. 1C, no. 5). Besides these long rod/spindle bacteria, PGN growth of small rod/coccus bacteria could also be readily observed (Fig. 1C, no. 6). Many of the classical growth and division modes of bacteria could be observed in the labeled gut microbiota, including diffuse synthesis of PGN (Fig. 2A), spiral synthesis (Fig. 2B), division dominated by septum synthesis (Fig. 2C), polar growth (Fig. 2D), and division by stalk/budding formation (Fig. 2E).

Identification of the bacterial growth patterns on the genus level

With the rich microbiological information obtained from the FDAA-labeled gut microbiota, taxonomically identifying individual bacterium in the view field became highly desirable. Toward this end, we resorted to FISH, a classical method for determining taxonomic information in complex bacterial samples. To facilitate the FISH probe selection and design, we first did 16S ribosomal DNA (rDNA)

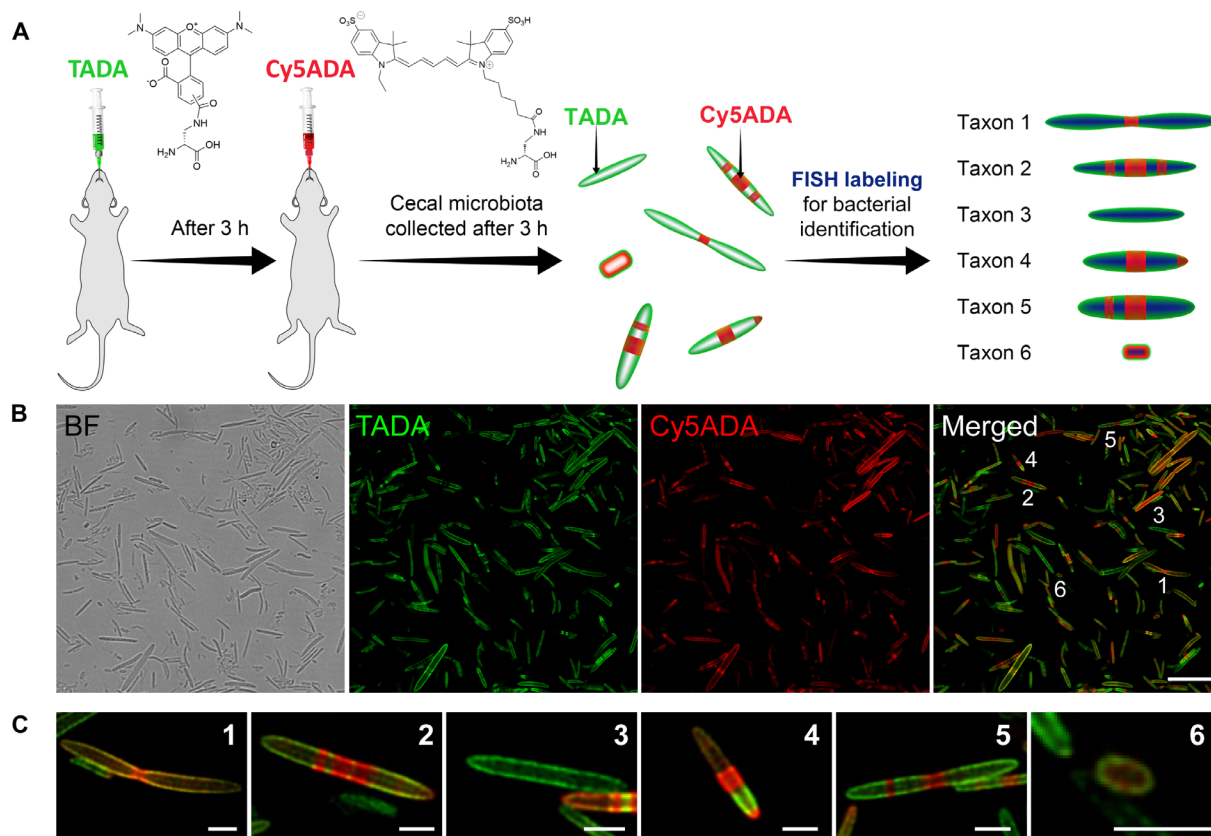


Fig. 1. Schematic illustration of the FDAA-based labeling strategy integrated with FISH staining and the two-color fluorescence imaging of the sequentially labeled gut microbiota. (A) TADA and Cy5ADA were given to mouse by gavage at an interval of 3 hours. The cecal microbiota was collected and imaged, and the taxonomic identifications of different bacteria were then determined by corresponding FISH probes. (B) Two-color fluorescence imaging of the gut bacteria sequentially labeled by TADA (green) and Cy5ADA (red). Scale bar, 10 μ m. Representative images from at least three independent experiments are shown. BF, Bright field. (C) Zoomed in view of the indicated bacteria from the merged image above. The green and red colors revealed the distinct growth patterns of different bacteria. Scale bars, 2 μ m.

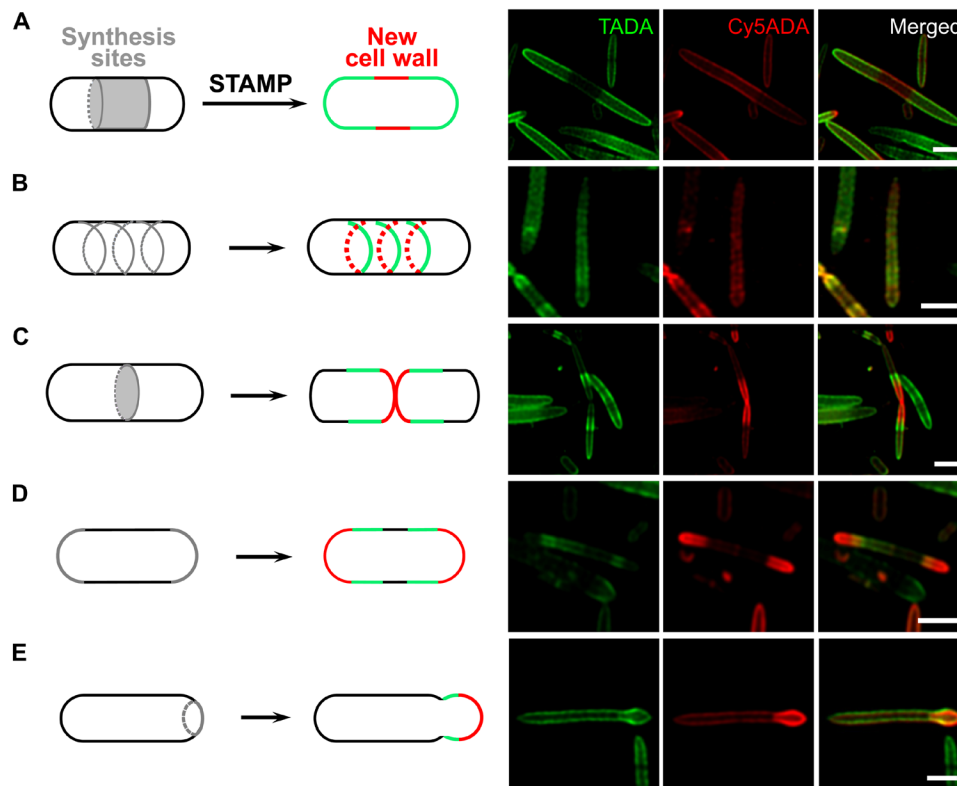


Fig. 2. Classical bacterial growth and division patterns could be observed in the labeled gut microbiota. Following STAMP (TADA and then Cy5ADA gavage), the mouse cecal microbiota was collected and analyzed by confocal fluorescence microscopy. In the cartoon, gray regions represent the sites of active cell wall synthesis, and green and red indicates the newly constructed PGN. (A) Diffuse synthesis of PGN. (B) Spiral synthesis of PGN. (C) Septum synthesis dominating the cell division. (D) Polar growth. (E) Stalk/budding formation. Scale bars, 2 μm .

and metagenomic sequencing of the labeled microbiotas (combined cecal microbiotas of five mice) to identify the bacterial composition (fig. S3 and table S2). To have a reasonably high coverage of the microbiota, we first used 15 FISH probes to stain some of the most abundant genera (covering ~71% of classified bacteria in the microbiota; table S1), the sequences of which were either based on previous reports or designed in this study. The FDAA-labeled microbiota was split into dozens of small aliquots and labeled by different FISH probes separately. It is worth mentioning that the microbiotas collected from small intestines also showed clear two-color FDAA labeling (fig. S4). However, because the amount of bacteria was very small, we did not perform any FISH staining.

Of the 15 FISH probes covering bacteria from nine families, seven stained Gram-positive and eight stained Gram-negative bacteria. Representative images of the labeled bacteria in each genus from multiple FISH experiments were presented. As expected, because of their thinner PGN, Gram-negative bacteria (Fig. 3, A to F) showed weaker FDAA labeling than the Gram-positive bacteria (Fig. 3, G to L), and most of them were short rods (1 to 2 μm). Of note, we also identified two Gram-negative genera, *Helicobacter* and *Desulfovibrio*, that could not be labeled by FDAAs (fig. S5). Extended labeling time (two gavages of TADA at an interval of 6 hours) still did not lead to any FDAA labeling (fig. S6). These bacteria may either have very slow PGN synthesis rates or have lipopolysaccharides/capsules impermeable to FDAA probes. It is also possible that they have atypical PGN structures or transpeptidases that cannot tolerate the incorporation of FDAAs, which merits further studies to extend our understanding of the structure and synthesis of PGN in different bacteria.

Most of the labeled Gram-positive bacteria (Fig. 3, G to L) were spindle shaped and divided by binary fission, but the distributions of the two colors in each genus were quite different, suggesting distinct arrangements of divisome and/or elongasome in various genera (11). For example, the bacteria shown in Fig. 3 (G to J) all belonged to the family *Lachnospiraceae*, but the two-color images presented different patterns. In *Lachnospiraceae incertae sedis* (LIS; Fig. 3G), FDAAs were labeled in a striped manner, but in *Lachnoclostridium* (Fig. 3H), *Roseburia* (Fig. 3I), and *Marvinbryantia* (Fig. 3J), the labeling was more diffuse. Moreover, we also identified some bacteria with polar growth, with one (Fig. 3F) or two poles (Fig. 3L) strongly labeled, a phenomenon that was previously only observed in some *Alphaproteobacteria* and *Actinobacteria* (12). The consistent bacterial labeling patterns and morphogenesis in each genus (fig. S7) also verified the specificities of the newly designed FISH probes. Of note, the specificities of several of the newly designed FISH probes could not be verified (listed in table S2). These probes either stained bacteria with inconsistent FDAA-labeling patterns or had a higher labeling ratio than the taxon's relative abundance determined by 16S rDNA sequencing. FISH sequences with improved specificities or a more stringent staining protocol are warranted for these bacterial groups.

Identification of the bacterial growth patterns on the species level

Of the 15 genera examined, *Clostridium* is known for being highly polyphyletic (13). We observed different labeling patterns within this

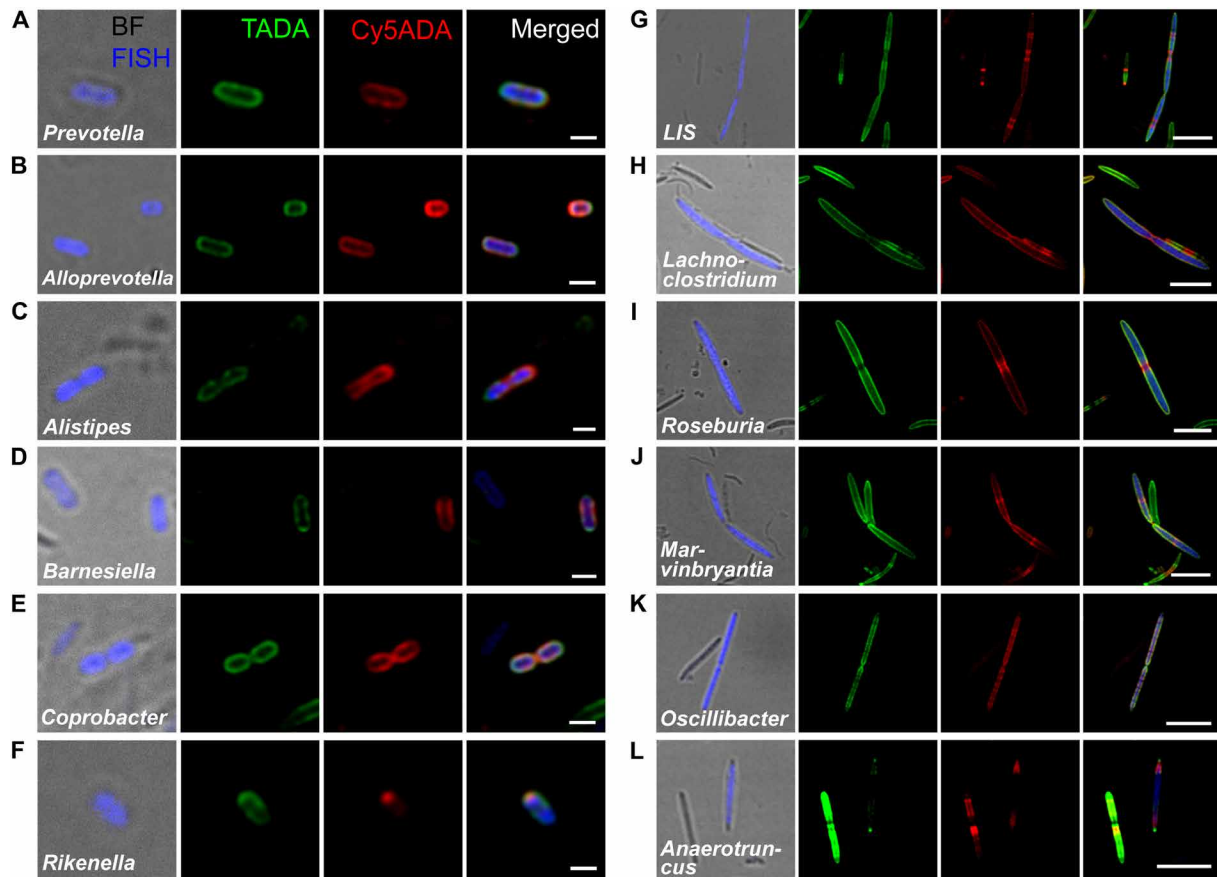


Fig. 3. Confocal fluorescence imaging of 12 FDAA-labeled and FISH-stained gut bacterial genera. The cecal microbiotas of mice received sequential labeling of TADA (green) and Cy5ADA (red) were stained by different FISH probes (blue) targeting corresponding genera. (A to F) Representative images of FDAA-labeled bacteria in six Gram-negative genera. Scale bars, 1 μm . (G to L) Representative images of FDAA-labeled bacteria in six Gram-positive genera. Scale bars, 5 μm . Photographs of bacteria, representing consistent labeling pattern in each genus from at least three independent FISH experiments, are presented.

genus (Fig. 4A). On the basis of the metagenomic sequencing results of the microbiota (table S2), we selected three species in this genus and labeled them with corresponding FISH probes designed for each. Varied labeling patterns were observed (Fig. 4B), with asymmetrical growth noticed in two (KNHs209 and ASF502) of the three species. Because *Clostridium* sp. ASF502 had never been cultured individually in vitro, these data showcased the potential of using our method for studying unculturable bacterial species in the gut microbiota.

Encouraged by the labeling results of *Clostridium*, we then set out to examine more species in the gut microbiota. Nine were selected, including six species that have been cultured in vitro: *Akkermansia muciniphila* (14), *Parabacteroides distasonis* (15),

Alistipes putredinis (16), *Lactobacillus johnsonii* (17), *Lactobacillus brevis* (18), and segmented filamentous bacteria (SFB; *Candidatus Savagella*) (19); and three unculturable taxa: *Oscillibacter* sp. 1-3, *Eubacterium* sp. 14-2, and *Dorea* sp. 5-2. The growth patterns of *A. muciniphila*, *P. distasonis*, *A. putredinis*, *Oscillibacter* sp., *Eubacterium* sp., and *Dorea* sp. were readily identified by our method (Fig. 5, A to F). However, because of the difficulties of performing FISH with *Lactobacillus* (20), the required step of lysozyme digestion destroyed most of the FDAA labeling signals from the bacteria, leaving only labeled septums (fig. S8). An improved FISH protocol for *Lactobacillus*

is required for more effective analysis of these important gut bacteria by our method.

As a heavily studied species with fundamental functions of degrading mucin, producing bioactive molecules and immune modulation (21), *A. muciniphila* cells were clearly observed dividing by binary fission (Fig. 5A). The imaged short rods of *P. distasonis* did not seem to be dividing (Fig. 5B). *A. putredinis* showed strong labeling at one pole, indicative of its polar growth (Fig. 5C). The three species that could not be cultured in vitro belonged to the order *Clostridiales*. *Oscillibacter* (Fig. 5D) and *Eubacterium* (Fig. 5E) might have diffuse synthesis of PGN (scheme shown in Fig. 2A), but *Dorea* seemed to have a more prominent septum (Fig. 5F), the synthesis of which might dominate cell division (scheme shown in Fig. 2C). Consistent modes of labeling and cellular morphologies in each species were observed in each species (fig. S9), supporting the specificities of these new FISH probes.

Revealing the in vivo growth of SFB

Another group of bacteria worth special note is SFB. As one of the most extensively studied bacteria in gut microbiota, SFB have been found to be critical in the induction of T helper cell 17, alongside many other immunity-related effects (22, 23). In the $\sim 90\text{-}\mu\text{m}$ SFB shown here (Fig. 6), we could clearly see the FDAA-labeled segments differentiated

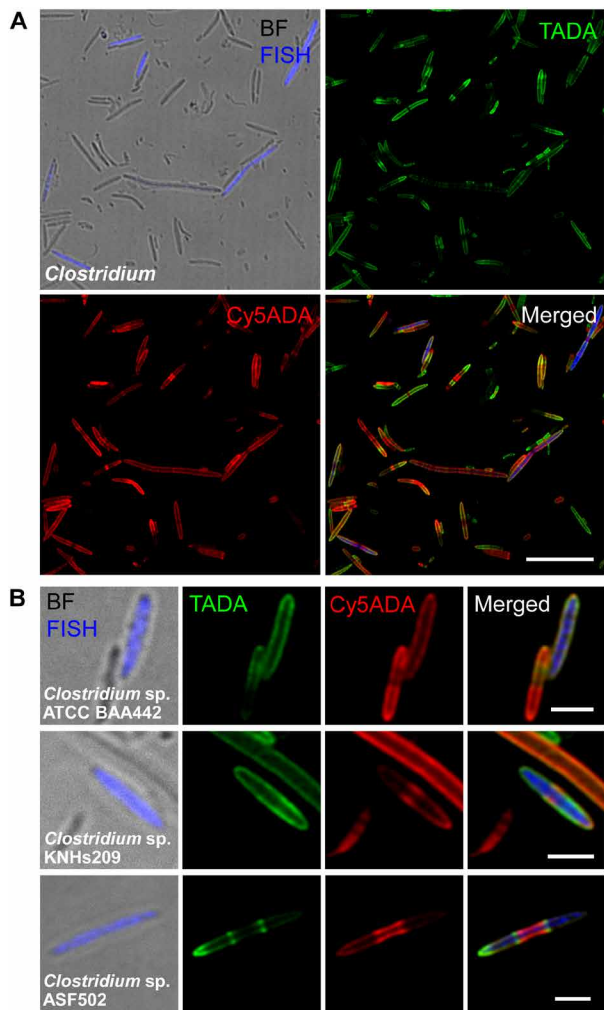


Fig. 4. *Clostridium* shows diverse cellular growth and division patterns. (A) Confocal fluorescence imaging of the polyphenotypic bacteria in the *Clostridium* genus identified by FISH staining. Scale bar, 10 μ m. (B) Three FISH probes targeting corresponding *Clostridium* species showed their distinct FDAA labeling patterns. Scale bars, 2 μ m. Photographs of bacteria, representing consistent labeling pattern in each species from at least three independent FISH experiments, are presented. ATCC, American Type Culture Collection.

at distinct stages (Fig. 6A), intrasegmental bodies (Fig. 6B), a needle-like holdfast (Fig. 6C), a triseptum at an asymmetric division location (Fig. 6C), and a symmetric division locus (Fig. 6D) (19). However, no obvious FDAA labeling of SFB intrasegmental bodies was noticed. Previously, it was reported that the PGN of *Bacillus subtilis* endospores lacked the D-Ala at the fifth locus of the peptide stem (24), which was the labeling target of FDAA in Gram-positive bacteria (7). This finding might explain the absence of FDAA labeling signals in SFB intrasegmental bodies. Of note, strong TADA and very weak Cy5ADA labeling were observed in the segments where intrasegmental bodies were found (Fig. 6, C and D, yellow arrows). This staining pattern suggests that metabolism of segmental PGN might be halted during formation of intrasegmental bodies, thus leading to reduced decay of the TADA signals (used in the first gavage) and much weaker labeling of Cy5ADA (used in the second gavage). Alternating intensities of the two colors were observed in

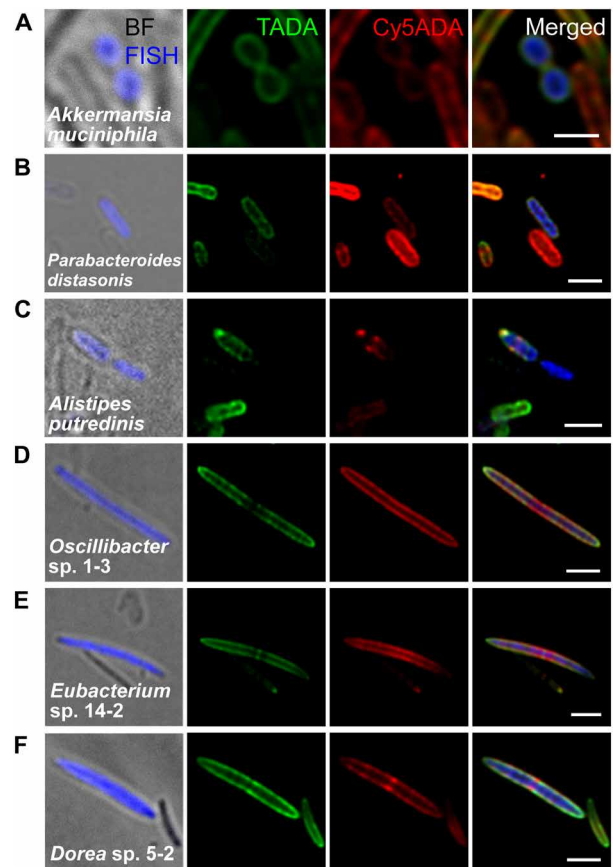


Fig. 5. Confocal fluorescence imaging of FDAA-labeled and FISH-stained gut bacterial species. The growth patterns of three species that are culturable in vitro (A to C) and three species that have not been cultured separately in the laboratory (D to F) are revealed. Scale bars, 2 μ m. Bacterial micrographs demonstrate consistent labeling patterns in each species from at least three independent FISH experiments.

some SFB cells on their neighboring septums (fig. S10). This pattern suggests that these segments were probably dividing during the two labeling steps, and that neighboring septums formed at different times were labeled with different concentrations of the two FDAAs. The phenotypes of SFB have been heavily studied mostly by scanning electron microscopy and Gram staining for nearly 50 years (25, 26). Our labeling strategy offers new perspectives on these important bacteria and will be a useful tool for further understanding the microbiology of SFB in vivo.

DISCUSSION

How PGN is constructed is one of the central topics in bacteriology. Sequential FDAA labeling has been used in investigating PGN synthesis in many model bacterial species (27). The strategy proposed here, to probe a large number of species in the microbiota collectively, greatly improves the efficiency of bacterial morphogenesis studies. Two-color imaging of the labeled gut microbiota recorded in situ growth and division patterns of the highly diverse gut bacteria during the 6 hours of labeling, giving us a unique opportunity for a direct look at how this “gut dark matter” actually grows and multiplies in vivo. The highly distinct labeling patterns of different gut bacteria offer a gold mine for microbial cytologists, where new bacterial

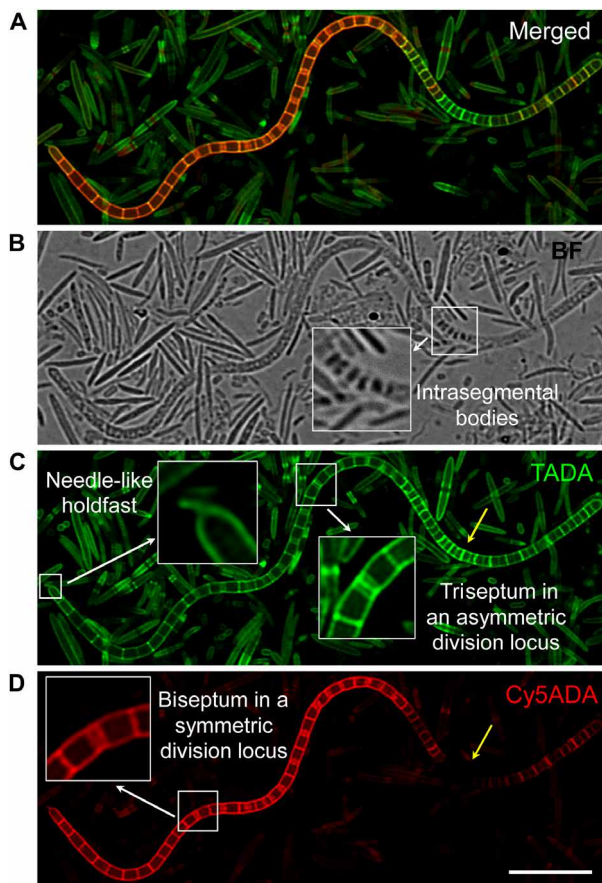


Fig. 6. Confocal fluorescence imaging of the sequentially labeled SFB. Some characteristic elements of SFB, including segments at varied differentiation stages (A), intrasegmental bodies (B), needle-like holdfast and triseptum in an asymmetric division location (C), and a symmetric division locus (D), were readily observed in the FDAA-labeled bacteria. Scale bar, 10 μ m.

growth and division patterns may be discovered. Moreover, FDAA-based visualization of several gut bacterial groups that have been heavily studied will enable further understanding of the activities of these important microbes in the mammalian gut. It is worth mentioning that among the 15 genera that were FDAA labeled, many species of *Prevotella*, *Roseburia*, *Oscillibacter*, *Anaerotruncus*, and *Barnesiella* were on the “most wanted” taxa list with high priority from the National Institutes of Health Human Microbiome Project (28). The information on in situ growth patterns captured by our method will provide valuable information about these understudied bacteria.

Further optimization of the FDAA probes, for instance, use of smaller fluorophores, for example, may improve labeling coverage, especially for those Gram-negative genera that could not yet be labeled. Optimized labeling protocols (e.g., varied time intervals between administration of the two probes) may assist characterization of the morphogenesis of different bacteria growing at different rates. Superresolution microscopy using FDAA-containing compatible fluorophores will also help in elucidating the distinct arrangements of PGN synthesis machineries in different bacteria, which will greatly enrich our knowledge of microbial cytology. Besides mouse gut the microbiota, studies of other complex microbial systems, such as the microbiota from other animal hosts and environmental microbiotas, including those in soil, water sediments, etc., may also benefit from this labeling and imaging strategy.

MATERIALS AND METHODS

Reagents

FDAA probe was purchased from Chinese Peptide Company (Hangzhou, China). FISH probes and paraformaldehyde were from Sangon Biotech (Shanghai, China). Other chemicals, not noted above, were from Sigma-Aldrich (St. Louis, MO, USA).

Animals

C57BL/6 specific pathogen-free mice (male, 6 weeks old) were obtained from Jie Si Jie Laboratory Animals (Shanghai, China). Mice were bred in the Renji Hospital animal facility in a temperature-controlled (25°C) environment with a 12-hour light/dark cycle, receiving a standard chow diet and free access to clean water. All animal experiments were performed in accordance with guidelines approved by the Institutional Animal Care and Use Committee of the Shanghai Jiao Tong University School of Medicine.

Sequential labeling of microbiotas with FDAA probes

The C57BL/6 mice were sequentially administered by two different FDAA probes (200 μ l, 1 mM TADA or Cy5ADA in distilled H₂O) through oral gavage with an interval of 3 hours. Their small intestine and cecal microbiotas were collected using a previously reported protocol (9). Briefly, mice were euthanized by cervical dislocation, and the small intestine and cecum were dissected separately and finely minced with a pair of 11.43-cm iris scissors in 1 ml of phosphate-buffered saline (PBS). The tissues and digesta were then filtered with a 40- μ m cell strainer to remove most of the nonbacterial materials. The filtrates were then centrifuged. The bacterial pellets (whitish-colored) were washed three times with 1.5 ml of PBS by centrifugation (15,000g, 3 min) and then resuspended in PBS for subsequent experiments.

In vitro culture of soil microbiota

Five grams of sediment collected from the Yangtze Estuary were homogeneously resuspended in 50 ml of sterile physiological water. Ten-fold serial dilutions of the sediment suspension were performed to 10⁻³. The serial dilutions (100 μ l) were dispersed on Gause's synthetic agar medium [containing 2% soluble starch, 0.1% KNO₃, 0.05% NaCl, 0.05% K₂HPO₄, 0.05% MgSO₄, 0.001% FeSO₄, and 2% agar (pH 7.2)] and then incubated at 30°C. After 3 days, bacterial cultures (10⁻²) with the most phenotypic diversity were collected, washed three times with 1.5 ml of PBS by centrifugation (15,000g, 3 min) and resuspended in sterile PBS for subsequent experiments.

FISH probe design

Candidate FISH probes were identified using a *k*-mer-based algorithm similar to KASpOD (29). The sequenced 16S ribosomal RNA (rRNA) genes were downloaded from the Ribosomal Database Project (RDP) (30) and SILVA (31) databases. Here, the missing 16S rDNA sequences of some target groups were downloaded from National Center for Biotechnology Information (32) and added manually. The final pool was consisted of 3,200,588 sequences. Target groups were defined as sequence subclasses consisted of 16S rDNA sequences from target family/genus. The nontarget groups were defined as sequence subclasses consist of 16S rDNA from nontarget bacteria, which located in the same order/family with targets. For each group, the fully overlapping *k*-mers were then clustered at an 88% identity clustering threshold to get the degenerate consensus *k*-mer. Coverage and specificity evaluation of each degenerate consensus *k*-mer from the target group were performed by a coverage assessment against the target and

nontarget groups, respectively. Consensus *k*-mers with best coverage and specificity was finally used as candidate probes. The related Perl scripts are available from <https://github.com/songjiajia2018/Pdesign/archive/master.zip>.

Probe optimization

The newly designed probes were added to the microbiota suspensions for test using probes EUB338 and NONEUB as positive and negative controls, respectively. There are a number of parameters that can be adjusted, such as temperature and formamide concentration, to choose the best stringency for hybridization. According to the method described by Manz *et al.* (33), varying the concentration of formamide in the hybridization buffer at a constant hybridization temperature (46°C), ranging from 0 to 70% (in 5% increments), was used to evaluate the optimal stringency of each probe designed in this study. Subsequently, an equally stringent 30 min posthybridization wash for each hybridization was performed at 48°C. Confocal or flow cytometry can be used to quantify the bacteria FISH signal intensity at different formamide concentrations. The highest formamide concentration before losing the specific hybridization signal was regarded as optimal hybridization stringency for the test probe.

To test the labeling specificities of the newly designed FISH sequences, the probes were separately tested against a fixed soil microbiota sample that did not share any genera with the mouse gut microbiota, using protocols described below. The presented 16 new FISH probes all showed negative labeling in the test (fig. S11). Further specificity confirmation tests were performed by flow cytometry and confocal fluorescence imaging. Flow cytometry was carried out to analyze the labeling ratios of some genera (*Clostridium*, *Barnesiella*, and *Alloprevotella*) in the microbiota, using a previously published method (34). These tests showed results consistent with their relative abundances deduce by 16S rDNA sequencing (fig. S12), indicative of high labeling specificities. Other genera and species tagged with the new FISH probes were analyzed by confocal fluorescence microscopy to assess whether the cell morphologies and labeling patterns of the stained bacteria were consistent in each group, which could further verify the specificities of the new FISH probes.

Fluorescence in situ hybridization

An equal volume of 4% paraformaldehyde was added to the bacterial suspensions in PBS and incubated at room temperature for 1.5 hours to fix the bacteria. The samples were then washed twice with PBS and resuspended in 50% ethanol-PBS (v/v) and stored at -20°C for >24 hours. After washing with PBS, the bacterial pellets were resuspended in a hybridization buffer [0.9 M NaCl, 20 mM tris (pH 7.5), 0.01% SDS, and formamide, if required] (table S1). The FISH probe was then added with a final concentration of 5 ng/μl and incubated overnight at required temperature (table S1) using a ThermoMixer (Eppendorf, Hamburg, Germany). After hybridization, bacteria were then washed two times (15 min) with washing buffer [0.9 M NaCl, 20 mM tris (pH 7.5), and 0.01% SDS]. Bacteria were then resuspended in tris buffer [20 mM tris and 25 mM NaCl (pH 7.5)] before analysis with fluorescence microscopy and flow cytometry. FISH probe sequences that have been previously reported (35–44) are listed in table S1.

Confocal fluorescence microscopy

A bacterial suspension was added to an agarose layer [1.5% (w/v) in PBS, ~1-mm thick] and covered with a glass coverslip. Confocal

fluorescence imaging was performed on a TCS SP8 laser scanning confocal microscope (Leica, Solms, Germany). Samples were excited with 488 nm for FAM (carboxyfluorescein), 555 nm for TAMRA, and 639 nm for Cy5 fluors, and the emission was detected using the corresponding emission filters. Deconvolution of the images was performed using Huygens Essential Deconvolution software (Scientific Volume Imaging B.V., Hilversum, The Netherlands) using a theoretical point spread function.

Flow cytometry

Flow cytometry analyses of the FDAA-labeled microbiota samples were carried out on a CytoFLex flow cytometer (Beckman Coulter Life Sciences, Indianapolis, IN, USA). FlowJo (V 10.0.8r1) was used for data analyses. Labeled microbiota were identified with flow cytometry plots of logFSC versus logSSC and then gated on fluorescence. For each sample, 15,000 events were collected for analysis with debris and doublets excluded.

Sequencing analysis

DNA from the microbiotas was extracted either using a stool DNA Kit or bacterial DNA Kit (Omega Bio-tek, Norcross, GA, USA) according to the manufacturer's protocol. The 16S rDNA sequencing and metagenomic sequencing were performed by Majorbio Bio-Pharm Technology Co. Ltd. (Shanghai, China). For 16S rDNA sequencing, the V3-V4 hypervariable regions of the 16S rDNA were amplified by polymerase chain reaction and subsequently paired-end sequenced (2 × 300) on an Illumina MiSeq platform (Illumina, San Diego, USA) according to the standard protocols. The taxonomy of each 16S rRNA gene sequence was analyzed by RDP Classifier (<http://rdp.cme.msu.edu/>) against the SILVA (SSU123) 16S rDNA database with a confidence threshold of 80%. For metagenomic sequencing, DNA was fragmented to an average size of about 400 bp using Covaris M220 (Gene Company Limited, China) for paired-end library construction and subsequently paired-end sequenced on an Illumina HiSeq4000 platform. BLASTP (Version 2.2.28+, <http://blast.ncbi.nlm.nih.gov/Blast.cgi>) was used for taxonomic annotations by aligning non-redundant gene catalogs against the integrated NR (non-redundant protein sequence) database with *e*-value cutoff of 1×10^{-5} .

SUPPLEMENTARY MATERIALS

Supplementary material for this article is available at <http://advances.sciencemag.org/cgi/content/full/6/36/eabb2531/DC1>

[View/request a protocol for this paper from Bio-protocol.](#)

REFERENCES AND NOTES

1. T. S. B. Schmidt, J. Raes, P. Bork, The human gut microbiome: From association to modulation. *Cell* **172**, 1198–1215 (2018).
2. A. Almeida, A. L. Mitchell, M. Boland, S. C. Forster, G. B. Gloor, A. Tarkowska, T. D. Lawley, R. D. Finn, A new genomic blueprint of the human gut microbiota. *Nature* **568**, 499–504 (2019).
3. C. Rinke, P. Schwientek, A. Sczyrba, N. N. Ivanova, I. J. Anderson, J. F. Cheng, A. Darling, S. Malfatti, B. K. Swan, E. A. Gies, J. A. Dodsworth, B. P. Hedlund, G. Tsiamis, S. M. Sievert, W. T. Liu, J. A. Eisen, S. J. Hallam, N. C. Kyrpides, R. Stepanauskas, E. M. Rubin, P. Hugenholtz, T. Woyke, Insights into the phylogeny and coding potential of microbial dark matter. *Nature* **499**, 431–437 (2013).
4. J. C. Lagier, G. Dubourg, M. Million, F. Cadoret, M. Bilen, F. Fenollar, A. Levasseur, J. M. Rolain, P. E. Fournier, D. Raoult, Culturing the human microbiota and culturomics. *Nat. Rev. Microbiol.* **16**, 540–550 (2018).
5. J. S. Biteen, P. C. Blainey, Z. G. Cardon, M. Chun, G. M. Church, P. C. Dorrestein, S. E. Fraser, J. A. Gilbert, J. K. Jansson, R. Knight, J. F. Miller, A. Ozcan, K. A. Prather, S. R. Quake, E. G. Ruby, P. A. Silver, S. Taha, G. van den Engh, P. S. Weiss, G. C. Wong, A. T. Wright, T. D. Young, Tools for the microbiome: Nano and beyond. *ACS Nano* **10**, 6–37 (2016).

6. D. Berry, B. Stecher, A. Schintlmeister, J. Reichert, S. Brugiroux, B. Wild, W. Wanek, A. Richter, I. Rauch, T. Decker, A. Loy, M. Wagner, Host-compound foraging by intestinal microbiota revealed by single-cell stable isotope probing. *Proc. Natl. Acad. Sci. U.S.A.* **110**, 4720–4725 (2013).
7. E. Kuru, H. V. Hughes, P. J. Brown, E. Hall, S. Tekkam, F. Cava, M. A. de Pedro, Y. V. Brun, M. S. VanNieuwenhze, *In situ* probing of newly synthesized peptidoglycan in live bacteria with fluorescent D-amino acids. *Angew. Chem. Int. Ed.* **51**, 12519–12523 (2012).
8. Y. P. Hsu, G. Booher, A. Egan, W. Vollmer, M. S. VanNieuwenhze, D-amino acid derivatives as *in situ* probes for visualizing bacterial peptidoglycan biosynthesis. *Acc. Chem. Res.* **52**, 2713–2722 (2019).
9. W. Wang, L. Lin, Y. Du, Y. Song, X. Peng, X. Chen, C. J. Yang, Assessing the viability of transplanted gut microbiota by sequential tagging with D-amino acid-based metabolic probes. *Nat. Commun.* **10**, 1317 (2019).
10. J. E. Hudak, D. Alvarez, A. Skelly, U. H. von Andrian, D. L. Kasper, Illuminating vital surface molecules of symbionts in health and disease. *Nat. Microbiol.* **2**, 17099 (2017).
11. A. J. Egan, R. M. Cleverley, K. Peters, R. J. Lewis, W. Vollmer, Regulation of bacterial cell wall growth. *FEBS J.* **284**, 851–867 (2017).
12. P. J. B. Brown, D. T. Kysela, Y. V. Brun, Polarity and the diversity of growth mechanisms in bacteria. *Semin. Cell Dev. Biol.* **22**, 790–798 (2011).
13. D. H. Parks, M. Chuvochina, D. W. Waite, C. Rinke, A. Skarshewski, P. A. Chaumeil, P. Hugenholtz, A standardized bacterial taxonomy based on genome phylogeny substantially revises the tree of life. *Nat. Biotechnol.* **36**, 996–1004 (2018).
14. M. Derrien, E. E. Vaughan, C. M. Plugge, W. M. de Vos, *Akkermansia muciniphila* gen. nov., sp. nov., a human intestinal mucin-degrading bacterium. *Int. J. Syst. Evol. Microbiol.* **54**, 1469–1476 (2004).
15. M. Sakamoto, Y. Benno, Reclassification of *Bacteroides distasonis*, *Bacteroides goldsteinii* and *Bacteroides merdae* as *Parabacteroides distasonis* gen. nov., comb. nov., *Parabacteroides goldsteinii* comb. nov. and *Parabacteroides merdae* comb. nov. *Int. J. Syst. Evol. Microbiol.* **56**, 1599–1605 (2006).
16. M. Rautio, E. Eerola, M. L. Vaisanen-Tunkelrott, D. Molitoris, P. Lawson, M. D. Collins, H. Jousimies-Somer, Reclassification of *Lactobacillus putredinis* (Weinberg et al., 1937) in a new genus *Alistipes* gen. nov., as *Alistipes putredinis* comb. nov., and description of *Alistipes finegoldii* sp. nov., from human sources. *Syst. Appl. Microbiol.* **26**, 182–188 (2003).
17. T. Fujisawa, Y. Benno, T. Yaeshima, T. Mitsuoka, Taxonomic study of the *Lactobacillus acidophilus* group, with recognition of *Lactobacillus gallinarum* sp. nov. and *Lactobacillus johnsonii* sp. nov. and synonymy of *Lactobacillus acidophilus* group A3 (Johnson et al. 1980) with the type strain of *Lactobacillus amylovorus* (Nakamura 1981). *Int. J. Syst. Bacteriol.* **42**, 487–491 (1992).
18. D. H. Bergey, R. S. Breed, B. W. Hammer, F. M. Huntoon, E. G. D. Murray, F. C. Harrison. *Bergey's Manual of Determinative Bacteriology* (Williams & Wilkins, Baltimore, MD, ed. 4, 1934)
19. P. Schnupf, V. Gaboriau-Routhiau, M. Gros, R. Friedman, M. Moya-Nilges, G. Nigro, N. Cerf-Bensussan, P. J. Sansonetti, Growth and host interaction of mouse segmented filamentous bacteria *in vitro*. *Nature* **520**, 99–103 (2015).
20. H. J. M. Harmsen, P. Elfferich, F. Schut, G. W. Welling, A 16S rRNA-targeted probe for detection of lactobacilli and enterococci in faecal samples by fluorescent *in situ* hybridization. *Microb. Ecol. Health Dis.* **11**, 3–12 (2011).
21. P. D. Cani, W. M. de Vos, Next-generation beneficial microbes: The case of *Akkermansia muciniphila*. *Front. Microbiol.* **8**, 1765 (2017).
22. K. Atarashi, T. Tanoue, M. Ando, N. Kamada, Y. Nagano, S. Narushima, W. Suda, A. Imaoka, H. Setoyama, T. Nagamori, E. Ishikawa, T. Shima, T. Hara, S. Kado, T. Jinnohara, H. Ohno, T. Kondo, K. Toyooka, E. Watanabe, S. Yokoyama, S. Tokoro, H. Mori, Y. Noguchi, H. Morita, I. I. Ivanov, T. Sugiyama, G. Nunez, J. G. Camp, M. Hattori, Y. Umesaki, K. Honda, Th17 cell induction by adhesion of microbes to intestinal epithelial cells. *Cell* **163**, 367–380 (2015).
23. M. S. Ladinsky, L. P. Araujo, X. Zhang, J. Veltri, M. Galan-Diez, S. Soualhi, C. Lee, K. Irie, E. Y. Pinker, S. Narushima, S. Bandyopadhyay, M. Nagayama, W. Elhenawy, B. K. Coombes, R. P. Ferraris, K. Honda, I. D. Iliev, N. Gao, P. J. Bjorkman, I. I. Ivanov, Endocytosis of commensal antigens by intestinal epithelial cells regulates mucosal T cell homeostasis. *Science* **363**, eaat4042 (2019).
24. A. Atrih, P. Zollner, G. Allmaier, S. J. Foster, Structural analysis of *Bacillus subtilis* 168 endospore peptidoglycan and its role during differentiation. *J. Bacteriol.* **178**, 6173–6183 (1996).
25. C. P. Davis, D. C. Savage, Habitat, succession, attachment, and morphology of segmented, filamentous microbes indigenous to the murine gastrointestinal tract. *Infect. Immun.* **10**, 948–956 (1974).
26. D. G. Chase, S. L. Erlandsen, Evidence for a complex life cycle and endospore formation in the attached, filamentous, segmented bacterium from murine ileum. *J. Bacteriol.* **127**, 572–583 (1976).
27. A. D. Radkov, Y. P. Hsu, G. Booher, M. S. VanNieuwenhze, Imaging bacterial cell wall biosynthesis. *Annu. Rev. Biochem.* **87**, 991–1014 (2018).
28. A. A. Fodor, T. Z. DeSantis, K. M. Wylie, J. H. Badger, Y. Ye, T. Hepburn, P. Hu, E. Sodergren, K. Liolios, H. Huot-Creasy, B. W. Birren, A. M. Earl, The "most wanted" taxa from the human microbiome for whole genome sequencing. *PLOS ONE* **7**, e41294 (2012).
29. N. Parisot, J. Denonfoux, E. Dugat-Bony, P. Peyret, E. Peyretailade, KASpOD—a web service for highly specific and explorative oligonucleotide design. *Bioinformatics* **28**, 3161–3162 (2012).
30. J. R. Cole, Q. Wang, J. A. Fish, B. Chai, D. M. McGarrell, Y. Sun, C. T. Brown, A. Porras-Alfaro, C. R. Kuske, J. M. Tiedje, Ribosomal Database Project: Data and tools for high throughput rRNA analysis. *Nucleic Acids Res.* **42**, D633–D642 (2013).
31. C. Quast, E. Pruesse, P. Yilmaz, J. Gerken, T. Schweer, P. Yarza, J. Peplies, F. O. Glöckner, The SILVA ribosomal RNA gene database project: Improved data processing and web-based tools. *Nucleic Acids Res.* **41**, D590–D596 (2012).
32. P. A. Kitts, D. M. Church, F. Thibaud-Nissen, J. Choi, V. Hem, V. Sapojnikov, R. G. Smith, T. Tatusova, C. Xiang, A. Zherikov, M. DiCuccio, T. D. Murphy, K. D. Pruitt, A. Kimchi, Assembly: A resource for assembled genomes at NCBI. *Nucleic Acids Res.* **44**, D73–D80 (2015).
33. W. Manz, R. Amann, W. Ludwig, M. Wagner, K.-H. Schleifer, Phylogenetic oligodeoxynucleotide probes for the major subclasses of proteobacteria: Problems and solutions. *Syst. Appl. Microbiol.* **15**, 593–600 (1992).
34. L. Lin, J. Song, Q. Wu, Y. Du, J. Gao, Y. Song, C. Yang, W. Wang, Quantification of bacterial metabolic activities in the gut by D-amino acid-based *in vivo* labeling. *Angew. Chem. Int. Ed.* **59**, 11923–11926 (2020).
35. P. T. Sunde, I. Olsen, U. B. Göbel, D. Theegarten, S. Winter, G. J. Debelian, L. Tronstad, A. Moter, Fluorescence *in situ* hybridization (FISH) for direct visualization of bacteria in periapical lesions of asymptomatic root-filled teeth. *Microbiology* **149**, 1095–1102 (2003).
36. H. J. Harmsen, G. C. Raangs, T. He, J. E. Degener, G. W. Welling, Extensive set of 16S rRNA-based probes for detection of bacteria in human feces. *Appl. Environ. Microbiol.* **68**, 2982–2990 (2002).
37. A. W. Walker, S. H. Duncan, E. C. McWilliam Leitch, M. W. Child, H. J. Flint, pH and peptide supply can radically alter bacterial populations and short-chain fatty acid ratios within microbial communities from the human colon. *Appl. Environ. Microbiol.* **71**, 3692–3700 (2005).
38. D. Greuter, A. Loy, M. Horn, T. Rattei, probeBase—An online resource for rRNA-targeted oligonucleotide probes and primers: New features 2016. *Nucleic Acids Res.* **44**, D586–D589 (2016).
39. V. Chan, G. Crocetti, M. Grehan, L. Zhang, S. Danon, A. Lee, H. Mitchell, Visualization of *Helicobacter* species within the murine cecal mucosa using specific fluorescence *in situ* hybridization. *Helicobacter* **10**, 114–124 (2005).
40. L. Rigottier-Gois, V. Rochet, N. Garrec, A. Suau, J. Doré, Enumeration of *Bacteroides* species in human faeces by fluorescent *in situ* hybridisation combined with flow cytometry using 16S rRNA probes. *Syst. Appl. Microbiol.* **26**, 110–118 (2003).
41. S. H. Park, K. Itoh, Species-specific oligonucleotide probes for the detection and identification of *Lactobacillus* isolated from mouse faeces. *J. Appl. Microbiol.* **99**, 51–57 (2005).
42. N. Liao, Y. Yin, G. Sun, C. Xiang, D. Liu, H. D. Yu, X. Wang, Colonization and distribution of segmented filamentous bacteria (SFB) in chicken gastrointestinal tract and their relationship with host immunity. *FEMS Microbiol. Ecol.* **81**, 395–406 (2012).
43. R. I. Amann, B. J. Binder, R. J. Olson, S. W. Chisholm, R. Devereux, D. A. Stahl, Combination of 16S rRNA-targeted oligonucleotide probes with flow cytometry for analyzing mixed microbial populations. *Appl. Environ. Microbiol.* **56**, 1919–1925 (1990).
44. G. Wallner, R. Amann, W. Beisker, Optimizing fluorescent *in situ* hybridization with rRNA-targeted oligonucleotide probes for flow cytometric identification of microorganisms. *Cytometry* **14**, 136–143 (1993).

Acknowledgments

Funding: We are grateful to the National Natural Science Foundation of China (grants 21807070, 21735004, 21775128, and 21705024) and the Innovative Research Team of High-Level Local Universities in Shanghai (SSMU-ZLXC20180701) for financial support. **Author contributions:** L.L., W.W., and C.Y. designed the study. L.L., Q.W., J.S., Y.D., and J.G. performed and analyzed experiments. Y.S. contributed intellectually to the analysis and interpretation of the data. L.L., W.W., and C.Y. wrote the manuscript. **Competing interests:** The authors declare that they have no competing interests. **Data and materials availability:** The 16S rDNA and shotgun sequencing data of the cecal microbiotas have been deposited in the Sequence Read Archive with BioSample accessions SAMN14694443 and SAMN14694444, respectively. In addition, the 16S rDNA sequencing data of the soil microbiota cultured *in vitro* has also been deposited in the Sequence Read Archive with BioSample accession SAMN14734540. Additional data related to this paper may be requested from the corresponding authors.

Submitted 11 February 2020

Accepted 13 July 2020

Published 4 September 2020

10.1126/sciadv.abb2531

Citation: L. Lin, Q. Wu, J. Song, Y. Du, J. Gao, Y. Song, W. Wang, C. Yang, Revealing the *in vivo* growth and division patterns of mouse gut bacteria. *Sci. Adv.* **6**, eabb2531 (2020).